Journal of Engineering Mathematics **37:** 11–25, 2000.

Deformations of carbon-fiber-reinforced yacht masts

D. CLEMENTS and T. COOKE
Department of Applied Mathematics, The University of Adelaide, Australia.
e-mail: dclement@maths.adelaide.edu.au tcooke@maths.adelaide.edu.au

Received 27 October 1998; accepted in revised form 15 July 1999

Abstract. This paper provides an analysis of deformations of a carbon-fiber-reinforced layered cylindrical yacht mast. The mast is subjected to an axial compressive load and analytical expressions for the resulting stress fields are obtained. The analysis is used to predict the failure mode for a particular class of yacht masts.

Key words: fiber-reinforced materials, anisotropic, elasticity, buckling.

1. Introduction

This study is concerned with the design of carbon-fiber-reinforced cylinders for use in racing-yacht masts. The mast structures considered involve three cylindrical layers of the same fiber-reinforced composite with the fibers in adjacent layers having different orientations. An analysis of the stress fields in masts of this type is presented and the results used to determine the configuration of a three-layered fiber-reinforced mast structure which optimises the compressive load-carrying capacity of the mast.

The motivation for this study arose from a problem considered at the 1995 Australian Mathematics-In-Industry Study Group (MISG) [1]. The problem involved the manufacture of carbon-fiber-reinforced yacht masts for 'Moth' class yachts. The principal feature of these masts is that, with the fibers oriented along the axis, it is possible to produce a very light mast (typically of radius 23 mm and thickness 1 mm) which is capable of sustaining the considerable compressive loads imposed on it by the rigging wires which keep the mast in a straight vertical position. However, when masts constructed in this way are subjected to these axial compressive loads they are prone to fail due to the fact that the fibers are inclined to buckle out of the resin which binds them together in the composite material. The ability of the mast to sustain the compressive loads is enhanced by including in the mast structure very thin inner and outer fiber-reinforced layers of the same carbon-reinforced material but with the fibers aligned circumferentially rather than along the mast axis. These layers add to the weight of the mast and, since their principal purpose is to keep the fibers in the central layer in line, it is desirable to keep their width as small as possible. Thus, the specific problem is to determine, for a specified mast thickness, the best thickness of the inner and outer layers in order to optimise the compressive load carrying capacity of the 'Moth' type yacht mast.

At the 1995 MISG a preliminary analytical stress analysis of part of the problem was carried out by means of thin shell theory. Also, a more comprehensive numerical examination of the problem was carried out with the finite-element package MSC/NASTRAN. On the basis of these investigations some conclusions were drawn regarding the likely failure mode for 'Moth' type yacht masts.

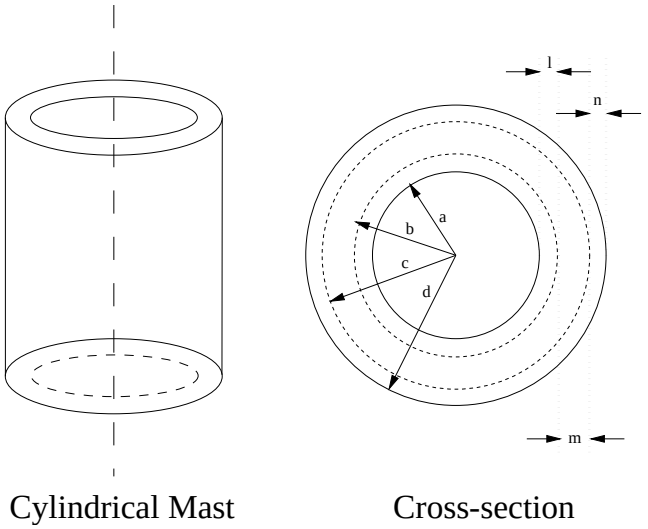

Figure 1. The geometry of the problem.

This paper is concerned with providing a more complete analytical analysis of the problem than was obtained at the MISG meeting and duly reported in the proceedings [1]. Specifically, an analytical examination of the stress field is presented without the thin-shell assumption and also a more complete thin-shell analysis is provided. In addition, an analytical consideration of the buckling of the mast structure is presented. These analytical results enable some conclusions to be drawn regarding the desirable width of the inner and outer layers for 'Moth'-type yacht masts. These conclusions obtained from the analytical examination of the problem are broadly in agreement with those obtained from the finite-element investigation reported in the MISG proceedings [1]

2. Statement of the problem

The problem described in the introduction may be specified more precisely as follows.

Referred to cylindrical polar coordinates r, θ, z consider a cylinder consisting of three layers with the axis of the cylinder along the z-axis (Figure 1). The middle layer of the cylinder lying between $r = b$ and $r = c$ $(0 < b < c)$ consists of a fibre-reinforced composite with the fibres parallel to the axis of the cylinder. The inner and the outer layers lying between $r = a$ and $r = b$ $(0 < a < b)$ and between $r = c$ and $r = d$ $(d > c)$ consist of the same fibre-reinforced composite with the fibres running in circles around the axis of the cylinder. The total thickness of the three layers is small relative to the mast radius.

A compressive load is applied to the cylinder in a direction parallel to the z-axis. The entire axial load is taken up by the middle layer (so the axial loads in the inner and outer layers are zero). It is required to find the stress and displacement throughout the cylinder and to determine the failure loads for compressive failure and also for failure due to local buckling.

For the purpose of this analysis, each layer is modelled by a homogeneous anisotropic elastic material with appropriate elastic constants used to reflect accurately the properties of the fibre-reinforced composite.

3. Notation and material constants

With minor modifications the notation used will follow that employed in the 1995 MISG proceedings [1].

r, θ, z = cylindrical polar coordinates
a = radius of inner surface
b = radius of interface between inner and middle layers
c = radius of interface between middle and outer layers
d = radius of outer surface
l = width of inner layer
m = width of middle layer
n = width of outer layer
E_l = Young's modulus in the fiber direction
E_t = Young's modulus transverse to the fibres
ν_{lt} = Poisson's ratio coupling strain in the fiber direction to strain normal to the fiber
ν_{tl} = Poisson's ratio coupling strain normal to the fiber to strain in the fiber direction
ν_{tt} = Poisson's ratio coupling strain in two orthogonal directions normal to the fiber
σ_{zz} = normal stress in plane perpendicular to mast axis
σ_{rr} = radial stress
$\sigma_{\theta\theta}$ = circumferential stress
ε_{rr} = strain in radial direction
$\varepsilon_{\theta\theta}$ = circumferential strain
ε_{zz} = strain in longitudinal direction

superscript$^{(o,m,i)}$ = refers to the outer, middle or inner layers

The values of the material constants which will be used throughout the paper are those employed in the 1995 MISG [1] for the carbon-fiber-reinforced material used for the manufacture of 'Moth' type yacht masts. The values are

E_t = 8 GigaPascals
E_l = 125 GigaPascals
$\sigma_l^{\text{tensile strength}}$ = 2090 MegaPascals
$\sigma_t^{\text{tensile strength}}$ = 64 MegaPascals
$\sigma_l^{\text{compressive strength}}$ = 1717 MegaPascals
$\sigma_t^{\text{compressive strength}}$ = 210 MegaPascals
ν_{lt} $\approx$ 0·35
ν_{tl} $\approx$ 0·02.

4. Classical linear elastic analysis

In this section the classical linear elastic theory for an anisotropic body is applied to analyse the stress field in the three-layer tubular mast structure of Section 2.

Under the assumption that the stresses are independent of θ and z and with zero tractions on the boundaries $r = a$ and $r = d$ it may readily be shown that the only nonzero stresses are $\sigma_{rr}, \sigma_{\theta\theta}$ and σ_{zz}. These stresses must satisfy the equilibrium equation (see Malvern [2, pp. 667–669])

$$\frac{\partial \sigma_{rr}}{\partial r} + \frac{\sigma_{rr} - \sigma_{\theta\theta}}{r} = 0. \tag{1}$$

This equilibrium equation will be automatically satisfied if the stresses take the form

$$\sigma_{rr} = \frac{1}{r}\frac{\partial \phi}{\partial r}, \tag{2}$$

$$\sigma_{\theta\theta} = \frac{\partial^2 \phi}{\partial r^2}, \tag{3}$$

where $\phi = \phi(r)$ is a twice differentiable function of r. The relevant compatibility equation is (see Malvern [2])

$$\frac{\partial^2 \varepsilon_{\theta\theta}}{\partial r^2} - \frac{1}{r}\frac{\partial \varepsilon_{rr}}{\partial r} + \frac{2}{r}\frac{\partial \varepsilon_{\theta\theta}}{\partial r} = 0. \tag{4}$$

At this point it is convenient to consider the middle layer and the inner and outer layers separately.

4.1. MIDDLE LAYER

For this layer the stress-strain relations are of the form (see Saada [3, Chapters 8 and 9], Lekhnitskii [5, p. 66])

$$\varepsilon_{rr} = \frac{1}{E_t}\sigma_{rr} - \frac{\nu_{tt}}{E_t}\sigma_{\theta\theta} - \frac{\nu_{lt}}{E_l}\sigma_{zz}, \tag{5}$$

$$\varepsilon_{\theta\theta} = -\frac{\nu_{tt}}{E_t}\sigma_{rr} + \frac{1}{E_t}\sigma_{\theta\theta} - \frac{\nu_{lt}}{E_l}\sigma_{zz}, \tag{6}$$

$$\varepsilon_{zz} = -\frac{\nu_{tl}}{E_t}\sigma_{rr} - \frac{\nu_{tl}}{E_t}\sigma_{\theta\theta} + \frac{1}{E_l}\sigma_{zz}, \tag{7}$$

where the symmetry properties of the stiffness matrix require that

$$\frac{\nu_{tl}}{E_t} = \frac{\nu_{lt}}{E_l}. \tag{8}$$

Use of (2), (3), (5) and (6) in Equation (4) yields

$$\frac{\mathrm{d}^4\phi}{\mathrm{d}r^4} + \frac{2}{r}\frac{\mathrm{d}^3\phi}{\mathrm{d}r^3} - \frac{1}{r^2}\frac{\mathrm{d}^2\phi}{\mathrm{d}r^2} + \frac{1}{r^3}\frac{\mathrm{d}\phi}{\mathrm{d}r} = 0. \tag{9}$$

The general solution of this differential equation may be written in the form

$$\phi(r) = Ar^2\log(r) + B\log(r) + Cr^2 + D, \tag{10}$$

where A, B, C and D are arbitrary constants.

4.2. INNER AND OUTER LAYERS

For these layers the stress-strain relations are of the form

$$\varepsilon_{rr} = \frac{1}{E_t}\sigma_{rr} - \frac{\nu_{lt}}{E_l}\sigma_{\theta\theta} - \frac{\nu_{tt}}{E_t}\sigma_{zz}, \tag{11}$$

$$\varepsilon_{\theta\theta} = -\frac{\nu_{tl}}{E_t}\sigma_{rr} + \frac{1}{E_l}\sigma_{\theta\theta} - \frac{\nu_{tl}}{E_t}\sigma_{zz}, \tag{12}$$

$$\varepsilon_{zz} = -\frac{\nu_{tt}}{E_t} - \frac{\nu_{lt}}{E_l}\sigma_{\theta\theta} + \frac{1}{E_t}\sigma_{zz}. \tag{13}$$

Use of (2), (3), (11) and (12) in Equation (4) yields

$$\frac{1}{E_l}\frac{\mathrm{d}^4\phi}{\mathrm{d}r^4} + \frac{2}{E_l r}\frac{\mathrm{d}^3\phi}{\mathrm{d}r^3} - \frac{1}{E_t r^2}\frac{\mathrm{d}^2\phi}{\mathrm{d}r^2} + \frac{1}{E_t r^3}\frac{\mathrm{d}\phi}{\mathrm{d}r} = 0. \tag{14}$$

The general solution of differential equation (14) may be written in the form

$$\phi(r) = Ar^{1-\beta} + \mathrm{B}r^{1+\beta} + \mathrm{C}r^2 + D, \tag{15}$$

where $\beta = \sqrt{E_l/E_t}$. Use of (15) and (10) in the expressions for the stress (2) and (3) gives

$$\sigma_{rr}^{(i)} = A^{(i)}(1-\beta)r^{-1-\beta} + B^{(i)}(1+\beta)r^{-1+\beta} + 2C^{(i)}, \tag{16}$$

$$\sigma_{\theta\theta}^{(i)} = -A^{(i)}(1-\beta)\beta r^{-1-\beta} + B^{(i)}(1+\beta)\beta r^{-1+\beta} + 2C^{(i)}, \tag{17}$$

$$\sigma_{rr}^{(m)} = A^{(m)}(2\log(r)+1) + \frac{B^{(m)}}{r^2} + 2C^{(m)}, \tag{18}$$

$$\sigma_{\theta\theta}^{(m)} = A^{(m)}(2\log(r)+3) - \frac{B^{(m)}}{r^2} + 2C^{(m)}, \tag{19}$$

$$\sigma_{rr}^{(o)} = A^{(o)}(1-\beta)r^{-1-\beta} + B^{(o)}(1+\beta)r^{-1+\beta} + 2C^{(o)}, \tag{20}$$

$$\sigma_{\theta\theta}^{(o)} = -A^{(o)}(1-\beta)\beta r^{-1-\beta} + B^{(o)}(1+\beta)\beta r^{-1+\beta} + 2C^{(o)}, \tag{21}$$

where the (i), (m) and (o) superscripts denote the inner, middle and outer layers, respectively. The radial displacement in the layers can be derived by the use of the equations (see Malvern [2])

$$\frac{\partial u_r^{(i)}}{\partial r} = \varepsilon_{rr}^{(i)} = \frac{1}{E_t}\sigma_{rr}^{(i)} - \frac{\nu_{lt}}{E_l}\sigma_{\theta\theta}^{(i)} - \frac{\nu_{tt}}{E_t}\sigma_{zz}^{(i)},$$

$$\frac{\partial u_r^{(m)}}{\partial r} = \varepsilon_{rr}^{(m)} = \frac{1}{E_t}\sigma_{rr}^{(m)} - \frac{\nu_{tt}}{E_t}\sigma_{\theta\theta}^{(m)} - \frac{\nu_{lt}}{E_l}\sigma_{zz}^{(m)},$$

$$\frac{\partial u_r^{(o)}}{\partial r} = \varepsilon_{rr}^{(o)} = \frac{1}{E_t}\sigma_{rr}^{(o)} - \frac{\nu_{lt}}{E_l}\sigma_{\theta\theta}^{(o)} - \frac{\nu_{tt}}{E_t}\sigma_{zz}^{(o)}.$$

Substituting (16)–(21) in these equations and integrating, we have

$$u_r^{(i)} = \frac{1}{\beta^2 E_t}[A^{(i)}(\beta-1)r^{-\beta}(\beta+\nu_{lt}) + B^{(i)}(\beta+1)r^{\beta}(\beta-\nu_{lt}) + 2C^{(i)}\beta(\beta-\nu_{lt})r - \nu_{tt}\sigma_{zz}^{(i)}r\beta^2],$$

$$u_r^{(m)} = \frac{r}{E_t}[2A^{(m)}(1-\nu_{tt})(\log(r)-1) - \frac{B^{(m)}}{r^2}(1+\nu_{tt}) + A^{(m)}(1-3\nu_{tt}) + 2C^{(m)}(1-\nu_{tt})] - \frac{\nu_{lt}}{E_l}\sigma_{zz}^{(m)}r,$$

$$u_r^{(o)} = \frac{1}{\beta^2 E_t}[A^{(o)}(\beta-1)r^{-\beta}(\beta+\nu_{lt}) + B^{(o)}(\beta+1)r^{\beta}(\beta-\nu_{lt}) + 2C^{(o)}\beta(\beta-\nu_{lt})r - \nu_{tt}\sigma_{zz}^{(o)}r\beta^2].$$

The displacement u_θ may be obtained from the above equations and the relation $\partial u_\theta/\partial\theta = -u_r + r\varepsilon_{\theta\theta}$. To ensure the continuity of the displacement u_θ it is necessary to set

$$C^{(i)} = C^{(o)} = A^{(m)} = 0. \tag{22}$$

Thus the final expressions for the radial displacement and stress in each layer are

$$u_r^{(i)} = \frac{1}{E_t}\left[A^{(i)}\left(1-\frac{1}{\beta}\right)\left(1+\frac{\nu_{lt}}{\beta}\right)r^{-\beta} + B^{(i)}\left(1+\frac{1}{\beta}\right)r^{\beta}\left(1-\frac{\nu_{lt}}{\beta}\right)\right], \tag{23}$$

$$\sigma_{rr}^{(i)} = A^{(i)}(1-\beta)r^{-1-\beta} + B^{(i)}(1+\beta)r^{-1+\beta}, \tag{24}$$

$$\sigma_{\theta\theta}^{(i)} = \frac{\beta}{r}[-A^{(i)}(1-\beta)r^{-\beta} + B^{(i)}(1+\beta)r^{\beta}], \tag{25}$$

$$u_r^{(m)} = \frac{1}{E_t}\left[-(1+\nu_{tt})\frac{B^{(m)}}{r} + 2(1-\nu_{tt})C^{(m)}r\right] - \frac{\nu_{lt}}{E_l}\sigma_{zz}^{(m)}r, \tag{26}$$

$$\sigma_{rr}^{(m)} = \frac{B^{(m)}}{r^2} + 2C^{(m)}, \tag{27}$$

$$\sigma_{\theta\theta}^{(m)} = -\frac{B^{(m)}}{r^2} + 2C^{(m)}, \tag{28}$$

$$u_r^{(o)} = \frac{1}{E_t}\left[A^{(o)}\left(1-\frac{1}{\beta}\right)\left(1+\frac{\nu_{lt}}{\beta}\right)r^{-\beta} + B^{(o)}\left(1+\frac{1}{\beta}\right)r^{\beta}\left(1-\frac{\nu_{lt}}{\beta}\right)\right]. \tag{29}$$

$$\sigma_{rr}^{(o)} = A^{(o)}(1-\beta)r^{-1-\beta} + B^{(o)}(1+\beta)r^{-1+\beta}, \tag{30}$$

$$\sigma_{\theta\theta}^{(o)} = \frac{\beta}{r}[-A^{(o)}(1-\beta)r^{-\beta} + B^{(o)}(1+\beta)r^{\beta}]. \tag{31}$$

5. Solution of the problem

The boundary and interface conditions on $r = a, b, c, d$ are

$$\sigma_{rr}^{(i)} = 0 \quad \text{on } r = a \tag{32}$$

$$u_r^{(i)} = u_r^{(m)}, \qquad \sigma_{rr}^{(i)} = \sigma_{rr}^{(m)} \quad \text{on } r = b, \tag{33}$$

$$u_r^{(m)} = u_r^{(o)}, \qquad \sigma_{rr}^{(m)} = \sigma_{rr}^{(o)} \quad \text{on } r = c, \tag{34}$$

$$\sigma_{rr}^{(o)} = 0 \quad \text{on } r = d. \tag{35}$$

Use of (28) and (25) together with the boundary conditions (35) yields

$$A^{(i)}(1-\beta) + B^{(i)}(1+\beta)a^{2\beta} = 0,$$

$$A^{(i)}(1-\beta)b^{-1-\beta} + B^{(i)}(1+\beta)b^{-1+\beta} = \frac{B^{(m)}}{b^2} + 2C^{(m)}$$

$$A^{(i)}\left(1-\frac{1}{\beta}\right)b^{-\beta}\left(1+\frac{\nu_{lt}}{\beta}\right) + B^{(i)}\left(1+\frac{1}{\beta}\right)b^{\beta}\left(1-\frac{\nu_{lt}}{\beta}\right)$$
$$+(1+\nu_{tt})\frac{B^{(m)}}{b} - 2(1-\nu_{tt})C^{(m)}b + \frac{\nu_{lt}E_t}{E_l}\sigma_{zz}^{(m)}b = 0,$$

$$A^{(o)}(1-\beta)c^{-1-\beta} + B^{(o)}(1+\beta)c^{-1+\beta} = \frac{B^{(m)}}{c^2} + 2C^{(m)},$$

$$A^{(o)}\left(1-\frac{1}{\beta}\right)c^{-\beta}\left(1+\frac{\nu_{lt}}{\beta}\right) + B^{(o)}\left(1+\frac{1}{\beta}\right)\left(1-\frac{\nu_{lt}}{\beta}\right)c^{\beta}$$
$$+(1+\nu_{tt})\frac{B^{(m)}}{c} - 2(1-\nu_{tt})C^{(m)}c + \frac{\nu_{lt}E_t}{E_l}\sigma_{zz}^{(m)}c = 0,$$

$$A^{(o)}(1-\beta)d^{-1-\beta} + B^{(o)}(1+\beta)d^{-1+\beta} = 0.$$

Solving this set of six linear equations and substituting the result in (23) and (31) allows us to calculate the stress and radial displacements of any point on the mast. Some particular numerical results are given in Table 1. The elastic constants used in these calculations were those of the carbon-fiber-reinforced material used to construct 'Moth' type masts given in Section 3. Although the stress $\sigma_{\theta\theta}$ does vary throughout each layer, the variation is of no more than two per cent. For the purposes of presenting numerical results in Table 1 a single number corresponding to the average of the stresses $\sigma_{\theta\theta}$ on each layer's inner and outer boundaries has been used. Also, in the table the notation $\sigma_{rr}^{(i-m)}$ is used to denote the stress σ_{rr} at the interface $r = a + l$ between the inner and middle layer and $\sigma_{rr}^{(m-o)}$ to denote the stress σ_{rr} at the interface $r = a + l + m$ between the middle and outer layer.

6. Thin-shell approximation

The analysis and results of the previous section suggest that, since the variation in the circumferential stresses through the layers is small, a simpler analysis involving a thin-shell approximation may be instructive. The basis of this approximate technique is to assume that each of the layers of material are very thin and so the stress $\sigma_{\theta\theta}$ is approximately constant throughout the layer.

The radial stresses at each of the interfaces may be related to the circumferential stresses in the inner and outer layers by consideration of a small wedge subtended by an infinitesimally small angle $\mathrm{d}\theta$ as shown in Figure 2. Summation of the force components in the horizontal direction gives

$$\sigma_{rr}^{(m-o)}(a+l+m)\,\mathrm{d}\theta + 2\sigma_{\theta\theta}^{(o)}n\sin\left(\frac{\mathrm{d}\theta}{2}\right) = 0,$$

and since the angle $\mathrm{d}\theta$ is infinitesimal $\sin(\mathrm{d}\theta/2) \approx \mathrm{d}\theta/2$. Use of the fact that the layers are thin compared with the radius a yields

$$\sigma_{rr}^{(m-o)} \approx -\frac{n}{a}\sigma_{\theta\theta}^{(o)} \tag{36}$$

Table 1. Numerical results for the stresses in each layer due to a compressive force of 10 kN.

Dimensions (mm)				Stresses (MPa)					
a	l	m	n	$\sigma_{\theta\theta}^{(i)}$	$\sigma_{\theta\theta}^{(m)}$	$\sigma_{\theta\theta}^{(o)}$	$\sigma_{rr}^{(i-m)}$	$\sigma_{rr}^{(m-o)}$	$\sigma_{zz}^{(m)}$
23	0·25	0·5	0·25	2·25	−2·884	3·45	0·0245	−0·0375	−136
50	0·25	0·5	0·25	1·20	−1·334	1·46	0·0060	−0·0073	−63·0
100	0·25	0·5	0·25	0·63	−0·669	0·70	0·0016	−0·0017	−31·7
23	0·10	0·8	0·10	5·52	−1·510	6·56	0·0239	−0·0274	−84·7
50	0·10	0·8	0·10	2·70	−0·703	2·92	0·0054	−0·0057	−39.4
100	0·10	0·8	0·10	1·38	−0·353	1·44	0·0014	−0·0014	−19·8
23	0·02	0·97	0·01	16·3	−0·518	16·7	0·0142	−0·0073	−69·8
50	0·02	0·97	0·01	7·62	−0·239	7·71	0·0030	−0·0015	−32·5
100	0·02	0·97	0·01	3·84	−0·120	3·86	0.0008	−0·0004	−16·3

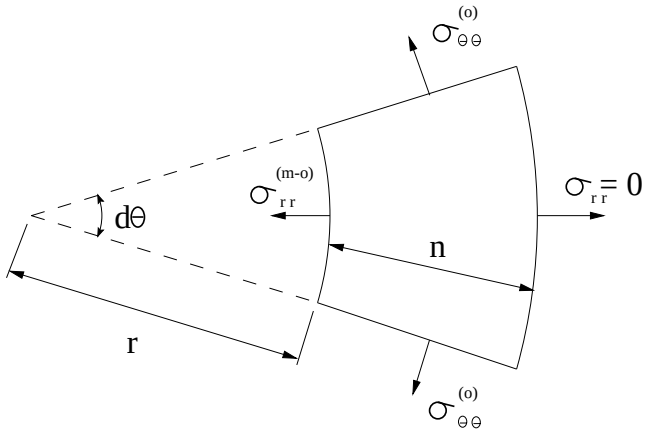

Figure 2. The forces acting on a single layer of a thin wedge.

and similarly for the inner layer

$$\sigma_{rr}^{(i-m)} \approx \frac{l}{a}\sigma_{\theta\theta}^{(i)}. \tag{37}$$

Now consider a small wedge containing all three layers as shown in Figure 3 where the boundary conditions require that the radial stresses σ_{rr} are zero on the inner and outer layers. Application of the equations of equilibrium to this infinitesimal wedge produces

$$\sigma_{\theta\theta}^{(i)} l + \sigma_{\theta\theta}^{(m)} m + \sigma_{\theta\theta}^{(o)} n = 0. \tag{38}$$

Since the material and the boundary conditions are both independent of θ, the deformed mast will maintain its circular cross-section. As a result, when the circumference increases in length by a certain percentage, the radius of the circular cross-section will increase by the

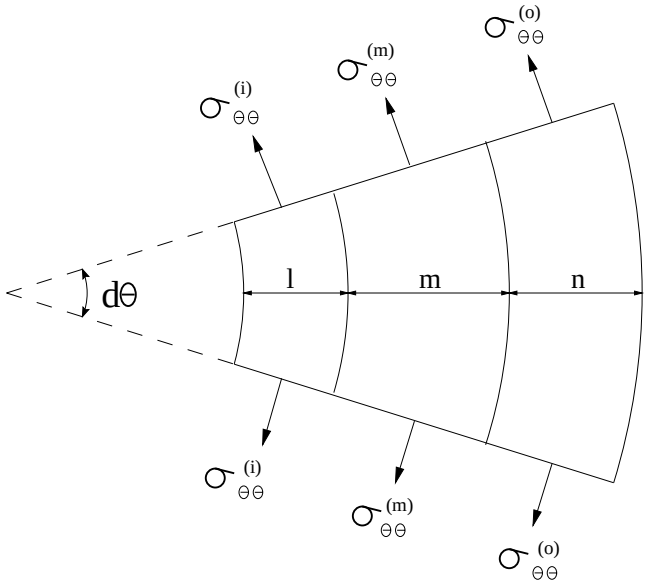

Figure 3. The forces acting on a thin wedge.

same percentage. Hence the strain $\varepsilon_{\theta\theta}$ must be continuous across each of the interfaces giving

$$\begin{aligned}\varepsilon^{(i)}_{\theta\theta} &= -\nu_{tl}\frac{\sigma^{(i)}_{zz}}{E_t} + \frac{\sigma^{(i)}_{\theta\theta}}{E_l} - \nu_{tl}\frac{\sigma^{(i-m)}_{rr}}{E_t} \\ &= -\nu_{lt}\frac{\sigma^{(m)}_{zz}}{E_l} + \frac{\sigma^{(m)}_{\theta\theta}}{E_t} - \nu_{tt}\frac{\sigma^{(i-m)}_{rr}}{E_t} \\ &= \varepsilon^{(m)}_{\theta\theta}. \end{aligned} \tag{39}$$

Since the inner and outer layers carry no axial stress (so $\sigma^{(i)}_{zz} = 0$), use of Equations (8) and (37) in (39) yields

$$\frac{\sigma^{(m)}_{\theta\theta}}{E_t} - \left[\frac{1}{E_l} + \frac{l}{a}\left(\frac{\nu_{tt}}{E_t} - \frac{\nu_{lt}}{E_l}\right)\right]\sigma^{(i)}_{\theta\theta} = \nu_{lt}\frac{\sigma^{(m)}_{zz}}{E_l}. \tag{40}$$

In a similar way consideration of the strain $\varepsilon_{\theta\theta}$ at the interface between the middle and outer layers yields

$$\frac{\sigma^{(m)}_{\theta\theta}}{E_t} - \left[\frac{1}{E_l} - \frac{n}{a}\left(\frac{\nu_{tt}}{E_t} - \frac{\nu_{lt}}{E_l}\right)\right]\sigma^{(o)}_{\theta\theta} = \nu_{lt}\frac{\sigma^{(m)}_{zz}}{E_l}. \tag{41}$$

If the thickness of the layers l and n are very much smaller than the radius of the mast a, then terms of order l/a and n/a may be ignored. Equations (40) and (41) then immediately provide

$$\sigma^{(i)}_{\theta\theta} = \sigma^{(o)}_{\theta\theta} \tag{42}$$

and then (38) and (40) (or (41)) yield, in turn,

$$\sigma^{(m)}_{\theta\theta} = -\frac{l+n}{m}\sigma^{(i)}_{\theta\theta}, \tag{43}$$

$$\sigma_{\theta\theta}^{(i)} = \sigma_{\theta\theta}^{(o)} = -\frac{\nu_{lt}}{[1 + \frac{l+n}{m}\frac{E_l}{E_t}]}\sigma_{zz}^{(m)}. \tag{44}$$

The solution to the three linear Equations (38), (40) and (41) provide a simple implicit solution for the stresses $\sigma_{\theta\theta}^{(i)}$, $\sigma_{\theta\theta}^{(m)}$ and $\sigma_{\theta\theta}^{(o)}$. Then Equations (36) and (37) may be used for calculation of the interfacial radial stresses and, hence, all of the stresses in each layer of the material for a given compressive load may be found. In the case when the layers l and m are very small compared with the radius a the explicit formulas (43) and (44) may be used to determine the circumferential stresses in place of Equations (38), (40) and (41). In particular, when l and n are small compared with the radius a, the formula (44) immediately shows that

$$\begin{aligned} |\sigma_{\theta\theta}^{(i)}| &= |\sigma_{\theta\theta}^{(o)}| \\ &< \nu_{lt}|\sigma_{zz}^{(m)}| \\ &= 0{\cdot}35|\sigma_{zz}^{(m)}|. \end{aligned}$$

Some particular numerical results obtained from these equations are given in Table 2, where use has been made of the elastic constants for the 'Moth' mast given in Section 3. Comparison of Tables 1 and 2 indicates that the results are in close agreement in the cases when the layer widths are much smaller than the radius a of the mast.

It is immediately clear for all the cases considered that the inner and outer layers will not fail in circumferential tension before the inner layer fails in longitudinal compression. Similarly, the middle layer will not fail in circumferential compression before it fails in longitudinal compression. For the case of very thin inner and outer layers ($l, n \approx 0$) Equations (44) and (45), taken together with the tensile and compressive strengths given in Section 3, indicate that in the circumferential direction the inner and outer layers are at approximately 29% of their tensile strength at the point when the inner layer fails in longitudinal compression.

Table 2. Numerical results for the stresses in each layer due to a compressive force of 10 kN.

Dimensions (mm)				Stresses (MPa)					
a	l	m	n	$\sigma_{\theta\theta}^{(i)}$	$\sigma_{\theta\theta}^{(m)}$	$\sigma_{\theta\theta}^{(o)}$	$\sigma_{rr}^{(i-m)}$	$\sigma_{rr}^{(m-o)}$	$\sigma_{zz}^{(m)}$
23	0·25	0·5	0·25	2·69	−2·852	3·01	0·0293	−0·0327	−136
50	0·25	0·5	0·25	1·29	−1·327	1·36	0·0065	−0·0068	−63·0
100	0·25	0·5	0·25	0·66	−0·667	0·68	0·0016	−0·0017	−31·7
23	0·10	0·8	0·10	5·91	−1·510	6·17	0·0257	−0·0268	−84·7
50	0·10	0·8	0·10	2·78	−0·703	2·84	0·0056	−0·0057	−39·4
100	0·10	0·8	0·10	1·41	−0·353	1·42	0·0014	−0·0014	−19·8
23	0·02	0·97	0·01	16·4	−0·509	16·5	0·0143	−0·0072	−69·8
50	0·02	0·97	0·01	7·65	−0·237	7·68	0·0031	−0·0015	−32·5
100	0·02	0·97	0·01	3·85	−0·119	3·86	0·008	−0·004	−16·3

The results indicate that, if 'Moth' type masts which are typically of radius 23 mm and thickness 1 mm were to fail due to compressive failure, the optimal design would be to have no inner or outer supporting layers at all. Practical tests indicate, however, that the load-bearing

capacity of the masts is improved by including thin inner and outer layers and this suggests that the main mode of failure of the 'Moth' mast is due to buckling.

7. Failure due to buckling

In this section the failure of the mast structure due to Euler and local buckling is considered

7.1. Euler buckling

The critical load for Euler buckling of a column, securely fixed at one end is expressed in Timoshenko and Gere [5, p. 48] as

$$F_{\mathrm{cr}} = \frac{\pi^2 E I}{4l^2}, \tag{45}$$

where l is the length of the column, E is Young's modulus along the length of the column and I is the moment of inertia about the bending axis. An equivalent flexural rigidity EI may be easily calculated for the three-layered cylinder to produce a critical load of

$$F_{\mathrm{cr}} = \frac{\pi^3(E_l(c^4 - b^4) + E_t(d^4 - c^4 + b^4 - a^4))}{8l^2}. \tag{46}$$

For the case of the 'Moth' mast (where $E_l > E_t$) for a given inner radius a and outer radius d this expression reaches a maximum when the inner and outer layers are both reduced to zero thickness (that is: $b = a$ and $c = d$). In practice, however, the 'Moth' mast would be constrained from buckling in this fashion by the rigging holding it straight and vertical. However, for other cylindrical columns with different properties and uses, this form of buckling may play an important role in determining its optimal dimensions.

7.2. Local buckling

Local buckling occurs when the walls of the cylindrical shell collapse without any bending about the axis of symmetry. The procedure described here calculates the failure load for the symmetrical buckling of the central load-bearing layer, taking into account the restorative forces of the inner and outer supportive layers. It does not take into account possible asymmetrical perturbations in either the applied compressive load, or the elastic properties of the materials. It also does not consider the possibility of asymmetric buckling. However, for a single-layered cylindrical shell, Timoshenko and Gere [5, p. 465] make the observation that the asymmetric buckling load is not greatly different from the symmetrical buckling load provided the cylinder is long enough. For this reason it is expected that the present analysis will provide a useful and accurate approximation to the exact buckling load.

The method to be used is similar to that outlined in Timoshenko and Gere [5, pp. 443–445]. Consider a thin strip taken out of the centre section, as shown in Figure 4. Each of these strips may be considered to act as single Euler columns with the local buckling of the cylinder corresponding to the Euler buckling of each strip about the XX-axis. The bending of each of these infinitesimal strips is governed by (see Timoshenko and Gere [5, p. 11])

$$EI\frac{\mathrm{d}^4 y}{\mathrm{d}x^4} + P\frac{\mathrm{d}^2 y}{\mathrm{d}x^2} = q(x), \tag{47}$$

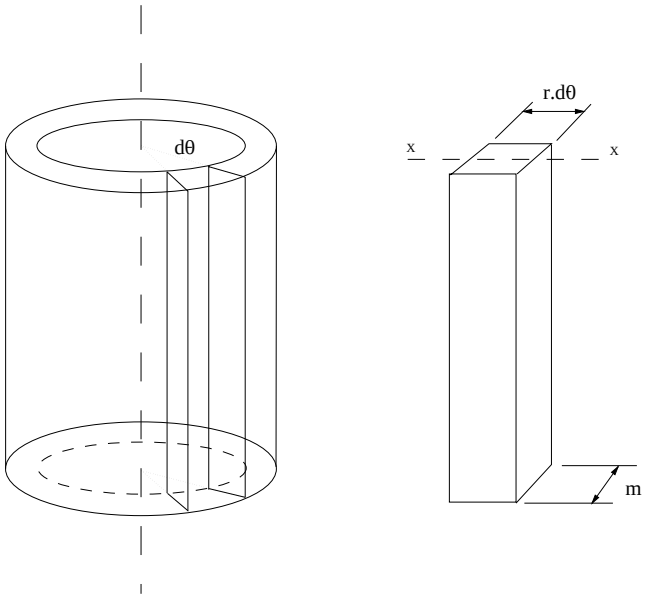

Figure 4. A thin strip taken from the central layer.

where E is Young's modulus in the longitudinal direction, I is the moment of inertia about the axis of bending, y is the horizontal displacement of the strip (which is dependent on x, the distance from the end of the strip), P is the axial force acting on the strip, and $q(x)$ is the restoring pressure.

If it is assumed that there is a force F acting uniformly over the entire middle layer, the force on the end of the strip will be

$$P = F\,\mathrm{d}\theta/(2\pi). \tag{48}$$

To produce an expression for the restoring force, it is assumed that the buckling is symmetric (so $y(x)$ is exactly the same for all of the strips).

At a distance x from the end of the mast, the central layer will buckle a distance $y(x)$. If the same assumptions are used as for the thin-shell approximation in Section 6, the stress $\sigma_{\theta\theta}^{(o)}$ in the outer layer is constant and according to Equation (36) is related to the interfacial stress $\sigma_{rr}^{(m-o)}$ at the interface $r = a + l + m$ by

$$\sigma_{\theta\theta}^{(o)} \approx -\frac{a}{n}\sigma_{rr}^{(m-o)}. \tag{49}$$

Since the layers are thin compared with the radius a, it follows that use of Equation (49) in Equation (12) provides

$$\sigma_{rr}^{(m-o)} \approx -\frac{n}{a}E_l\varepsilon_{\theta\theta}^{(o)} = -E_l\frac{ny}{a^2}. \tag{50}$$

If similar arguments are used for the other two layers (and if the argument that the middle layer is not compressed significantly is used, so that all three layers are displaced by the same $y(x)$), the following total restoring pressure (force per unit length) distribution results

$$q(x) = -\left[\frac{(l+n)y}{a^2}E_l + \frac{my}{a^2}E_t\right]a\,\mathrm{d}\theta. \tag{51}$$

Since the expression for the restoring force depends on $l + n$, but not l or n separately, the critical load for local buckling will depend on the total percentage of hoop reinforcement rather than the size of each of the individual hoop layers.

The relevant moment of inertia I for the column depicted in Figure 4 is given by

$$I = \frac{a\,\mathrm{d}\theta m^3}{12}\left[1 + \frac{2l+m}{2a}\right]. \tag{52}$$

Substitution of (48), (51), (52) in (47) now gives

$$E_l \frac{a\,\mathrm{d}\theta m^3}{12}\left[1 + \frac{2l+m}{2a}\right]\frac{\mathrm{d}^4 y}{\mathrm{d}x^4} + F\frac{\mathrm{d}\theta}{2\pi}\frac{\mathrm{d}^2 y}{\mathrm{d}x^2} + \left(\frac{l+n}{a}E_l + \frac{m}{a}E_t\right) y\,\mathrm{d}\theta = 0. \tag{53}$$

Hence

$$\frac{am^3}{12}\left[1 + \frac{2l+m}{2a}\right]\frac{\mathrm{d}^4 y}{\mathrm{d}x^4} + \frac{F}{2\pi E_l}\frac{\mathrm{d}^2 y}{\mathrm{d}x^2} + \left(\frac{l+n}{a} + \frac{E_t m}{E_l a}\right) y = 0. \tag{54}$$

This is a fourth-order, ordinary differential equation with constant coefficients which can be solved exactly. The solution will be of the form $y(x) = A\sin(w_1 x) + B\cos(w_1 x) + C\sin(w_2 x) + D\cos(w_2 x)$ where A, B, C and D are arbitrary constants which may be determined by boundary conditions at the ends of the mast. Imposing these boundary conditions provides a set of linear algebraic equations for the four constants A, B, C and D. The determinant of the coefficients in these linear algebraic equations becomes zero when $w_1 = w_2$ and this equation provides the criterion for buckling. Now from (54) the condition for buckling $w_1 = w_2$ leads to the following equation for the buckling load F_{cr}

$$\left[\frac{F_{\mathrm{cr}}}{2\pi E_l}\right]^2 - \frac{am^3}{3}\left[1 + \frac{2l+m}{2a}\right]\left[\frac{E_l(l+n) + E_t m}{E_l a}\right] = 0, \tag{55}$$

Since the layers are thin compared with the radius a, only leading terms involving layer thickness over the mast radius need to be retained, so that (55) reduces to

$$\left[\frac{F_{\mathrm{cr}}}{2\pi E_l}\right]^2 - \frac{am^3}{3}\left[\frac{E_l(l+n) + E_t m}{E_l a}\right] = 0, \tag{56}$$

which is independent of the radius of the mast. Rearranging this formula gives an explicit expression for the critical load

$$F_{\mathrm{cr}} = \frac{2}{\sqrt{3}}\pi E_l \sqrt{m^3\left((l+n) + \frac{E_t}{E_l}m\right)}. \tag{57}$$

The maximum buckling load will occur when

$$\frac{\partial F_{\mathrm{cr}}}{\partial m} = \left[2\sqrt{m^3\left((l+n) + \frac{E_t}{E_l}m\right)}\right]^{-1}\frac{\partial}{\partial m}\left[m^3\left(t + \left(\frac{E_t}{E_l} - 1\right)m\right)\right] = 0,$$

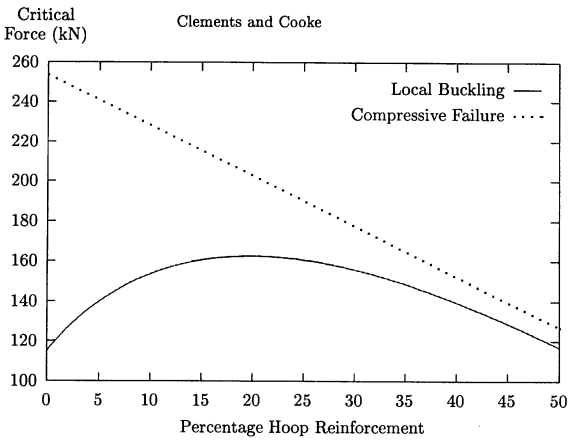

Figure 5. Comparison of critical loads.

where $t = l + m + n$ is the mast thickness. Therefore, for a mast of constant thickness t, the maximum buckling load will occur when

$$3t + 4m\left(\frac{E_t}{E_l} - 1\right) = 0. \tag{58}$$

For the specific case of the 'Moth'-type yacht mast, substituting the relevant material constants E_t and E_l from Section 3 in this expression gives $m = 0{\cdot}8013t$. Since the mast thickness is given by $t = l + m + n$, it immediately follows that the thickness of the inner and outer layers $l + n$ as a fraction of the total thickness is given by

$$\frac{l+n}{t} = 1 - \frac{m}{t} = 0{\cdot}1987. \tag{59}$$

A quick calculation of the critical force indicates that the failure load is in fact less for local buckling than for compressive failure, and hence from (59) the optimum hoop reinforcement is approximately 19·87% of the total thickness of the mast.

In Figure 5 the critical load for local buckling F_{cr} obtained from Equation (57) is plotted against the percentage of hoop reinforcement $100(l+n)/t$ for a typical 'Moth' mast for which the total thickness $t = l + m + n = 1\,\mathrm{mm}$ and the radius $a = 23\,\mathrm{mm}$. Also plotted on the same graph, with reference to the analysis of Section 4, is the compressive failure load for the same mast. It is apparent for all of the percentages of hoop reinforcement considered that the failure load due to local buckling is less than the compressive failure load. Thus, this analysis indicates that the failure mode for such masts is local buckling and to maximise the critical buckling load 19·87% of the total thickness should be hoop reinforcement.

8. Summary and conclusions

The analysis of this paper involved aspects of the deformation of a three-layered carbon-fiber-reinforced yacht mast such as would be found in 'Moth'-type yachts. In the analysis both failure under compression and local buckling have been examined and as a result, some design specification for masts of this type have been obtained. Specifically, for the type of

mast structure considered it has been shown that, to maximise the load at which failure occurs, roughly 20% of the mast thickness should consist of carbon-fiber-reinforced inner and outer layers with the fibers in these layers wound around the mast in planes normal to the mast axis. The results in Figure 5 indicate that the introduction of these layers into the mast structure increases the critical buckling load by approximately 30%.

No account has been taken of a number of factors which may also impinge upon the strength of the mast. For example, poor fabrication of the fiber-reinforced material, such that all the fibers in the central layer of the material are not all straight, may be an important factor in the strength of the mast (see Fleck [6]). Also, bending of the mast has not been considered in determining the critical load. The rigging supports would normally keep the mast straight and remove any bending effect, but in the event of any substantial bending occurring this could significantly affect the strength of the mast. Although these and other factors may be important in isolated cases, practical experience with particular 'Moth' masts indicates that, in general, this paper provides the relevant analysis of the major effects leading to the failure of masts of this type.

Acknowledgements

As indicated in the introduction the analysis in this paper follows on from a problem considered at the 1995 MISG conference [1]. At that conference a group of individuals considered the problem over a five-day period. The authors acknowledge the contribution of the MISG participants in identifying the essential features of the problem. In particular, the authors acknowledge the contribution of James Gunning who largely carried out the thin-shell analysis reported in [1] and thus provided the basic ideas for the more comprehensive thin-shell analysis of Section 5 of this paper. Also, the finite-element analysis carried out by David Rees in [1] is duly acknowledged, since it played an important role in reaching the essential conclusions at the MISG conference–conclusions which are now supported by the analytical analysis in this paper. The contribution of the co-moderator for the MISG project, Aaron Blichlau, is also acknowledged, together with the very substantial facilitative contribution of the Director of the 1995 MISG, Kerry Landman.

References

1. J. Hewitt, (ed.), Mechanical characteristics of carbon fiber yacht masts. In: *Proceedings of the Mathematics-In-Industry Study Group*. Adelaide: University of South Australia Document Services (1996) pp. 37–47.
2. L. E. Malvern, *Introduction to the Mechanics of a Continuous Medium*. Englewood Cliffs: Prentice Hall (1969) 713 pp.
3. A. Saada, *Elasticity: Theory and Applications*. New York: Pergamon (1974) 643 pp.
4. S. G. Lekhnitskii, *Theory of Elasticity of an Anisotropic Elastic Body*. San Francisco: Holden-Day (1963) 404 pp.
5. S. Timoshenko and J. Gere, *Theory of Elastic Stability*. New York: McGraw Hill (1961) 541 pp.
6. N. A. Fleck, Compressive failure of fiber composites. *Adv. Appl. Mech.* 33 (1997) 43–113.